

Monte Carlo simulations of ion transport in magnetic island regions

Rodrigo Saavedra and Julio J. Martinell

Instituto de Ciencias Nucleares, UNAM, A. Postal 70-543, México D.F., Mexico

I. Introduction. Confinement of fast ions is important to have efficient heating of fusion plasmas in the form of NBI and of alpha particles. It is known that magnetic islands may form in low-order rational magnetic surfaces in toroidal fusion devices which modify the magnetic geometry and should affect particle transport. It has been shown that rational surfaces may act as transport barriers for suprathermal electrons in electron cyclotron resonance heating (ECRH) experiments, [1] and thermal ions in stellarators such as TJ-II. Likewise, the fast ions resulting from neutral beam injection (NBI) interact with the magnetic islands altering their transport but the usual neoclassical transport analysis based on nested magnetic surfaces is not valid. Here we study the transport of a population of test particles in the presence of a magnetic island configuration produced by collisions with a Maxwellian plasma background consisting of electrons and a single species of ions, which are described by stochastic operators [3]. Particle orbits are obtained by numerically solving Langevin equations and transport coefficients are calculated with the Monte Carlo method from an ensemble of ions [2].

The equations are solved with a fourth order Runge-Kutta algorithm with a random choice of the sign in the Lorentz collision operators at each time step. Additionally a radial electric field was included, which modifies the transport of particles. The diffusion coefficient was calculated from the standard expression $D = \frac{1}{2tN} \sum_{j=1}^N (x_j(t) - x_j(0))^2$ where $x_j(t)$ is the position of a particle at time t .

II. Slab model The magnetic field model including islands is given by

$$\mathbf{B}(x, y, z) = \hat{\mathbf{z}} \times \nabla \psi + B_z \hat{\mathbf{z}}; \quad \psi = \psi_0 \log \cosh(x) + \psi_1 \cos(ky)$$

where ψ_0 represents the poloidal flux and $\psi_1 < \psi_0$ the strength of the island perturbation. The phase space variables used to describe the particle motion are $(\mathbf{r}, v^2, \lambda = v_{\parallel}/v)$ in terms of which the guiding center equations are

$$\begin{aligned} \frac{d\mathbf{r}}{dt} &= \mathbf{v}_{\parallel} + \mathbf{v}_D \\ \frac{dv^2}{dt} &= 2(\mathbf{v}_{\parallel} + \mathbf{v}_D) \cdot \mathbf{E} \\ \frac{d\lambda}{dt} &= \frac{1 - \lambda^2}{2} \left[\frac{2}{vv_{\parallel}} (\mathbf{v}_{\parallel} + \mathbf{v}_D) \cdot \mathbf{E} - \frac{v}{v_{\parallel} B} (\mathbf{v}_{\parallel} + \mathbf{v}_D) \cdot \nabla B \right], \end{aligned}$$

where v_{\parallel} and v_D are the usual parallel and drift velocities respectively. A constant electric field can also be included as $\mathbf{E} = E_0\hat{x}$.

These equations can be numerically integrated to obtain single particle trajectories. The effect of collisions is introduced through pitch-angle and energy scattering operators [3]

$$\begin{aligned}\lambda_n &= \lambda_0 - \sum_b v_d(b) \lambda_0 \tau \pm \left[\sum_b v_d(b) (1 - \lambda_0^2) \right]^{1/2} \tau^{1/2} \\ E_n &= E_0 - 2 \sum_b v_E(b) \left\{ E_0 - \frac{x(b)}{\pi^{1/2}} \frac{\exp[-x^2(b)]}{\Psi[x(b)]} T(b) \right\} \tau \pm 2 \left[\sum_b v(b) T(b) E_0 \right]^{1/2} \tau^{1/2}\end{aligned}\quad (1)$$

One effect of collisions is to produce transitions between trapped and passing particles. An initial population of N_0 particles starting at a fixed radius (x coordinate) is followed in time to determine the ensuing particle distribution. Figure 1 shows the ion distribution for $N_0 = 1000$ with initial kinetic energy taken from a Maxwellian of mean 1 keV located near the separatrix of an $m = 2$ island configuration and followed for 3 ms (about 5 collision times), within the range $-a/2 < x < a/2, -\pi a < y < \pi a, -\pi R < z < \pi R$ with periodic boundary conditions in y and z which represent the poloidal and toroidal coordinates, respectively.

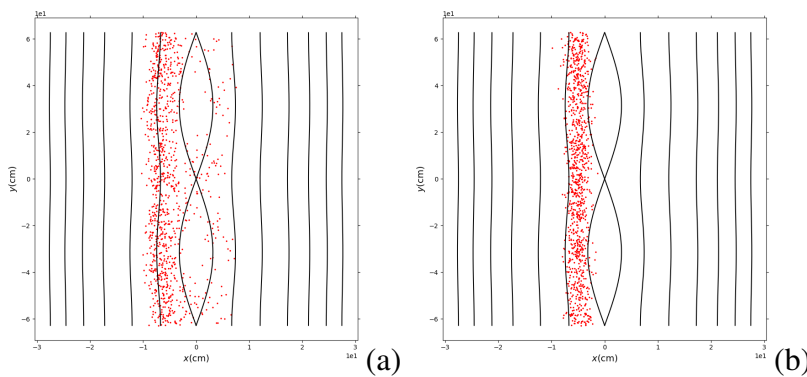


Figure 1: Final distribution with $\phi = 0$ (a) and $\phi = 8kV$ (b).

From Fig. 1a it can be seen that few particles trespass the islands region, displaying a barrier effect on transport. The same simulation was carried out but with an electric field corresponding to a potential of 8 kV, it can be seen from Fig.

1b that particles are better confined in this case. From the variance σ^2 of the ion distribution as function of time the diffusion coefficient can be computed as $D = \sigma^2/2t$. It is found that $D = 3600\text{cm}^2/\text{s}$ and $D = 3.76\text{cm}^2/\text{s}$ without and with E -field, respectively.

III. Tokamak model The model equilibrium normalized magnetic field used is [6]

$$B(r, \theta, \zeta) = 1 - \varepsilon_t \cos \theta - \varepsilon_h \cos \eta (1 - \cos \theta) \quad (2)$$

where $\eta = l\theta - j\zeta$; for a tokamak we take $\varepsilon_h = 0$. The magnetic island is represented by a perturbation to the equations $\delta\mathbf{B} = \nabla \times \alpha \mathbf{B}$; $\alpha = \alpha_{mn} \sin(m\theta - n\zeta)$, ($s = q'/q$) which produces a magnetic island at ψ_p with $q(\psi_p) = m/n$, of width $\Delta = 4\sqrt{\alpha_{mn}/s}$.

The phase-space variables are $(\psi_p, \theta, \zeta, \rho_{\parallel})$, with $\psi_p = B_0 r^2 / 2$ the poloidal flux, θ, ζ poloidal/toroidal angles and $\rho_{\parallel} = v_{\parallel} / B$. The guiding center equations are [4]

$$\begin{aligned}\dot{\psi}_p &= -\frac{g}{D} \left[(\mu + \rho_{\parallel}^2 B) \partial_{\theta} B + \partial_{\theta} \Phi \right] + \frac{I}{D} \left[(\mu + \rho_{\parallel}^2 B) \partial_{\zeta} B + \partial_{\zeta} \Phi \right] + \frac{g \rho_{\parallel} B^2}{D} \partial_{\theta} \alpha - \frac{I \rho_{\parallel} B^2}{D} \partial_{\zeta} \alpha \\ \dot{\theta} &= \frac{\rho_{\parallel} B^2}{D} (1 - \rho_c g' - g \partial_{\psi_p} \alpha) + \frac{g}{D} \left[(\mu + \rho_{\parallel}^2 B) \partial_{\psi_p} B + \partial_{\psi_p} \Phi \right] \\ \dot{\zeta} &= \frac{\rho_{\parallel} B^2}{D} (q + \rho_c I' + I \partial_{\psi_p} \alpha) - \frac{I}{D} \left[(\mu + \rho_{\parallel}^2 B) \partial_{\psi_p} B + \partial_{\psi_p} \Phi \right] \\ \dot{\rho}_{\parallel} &= \frac{1}{D} (I \partial_{\zeta} \alpha - g \partial_{\theta} \alpha) \left[(\mu + \rho_{\parallel}^2 B) \partial_{\psi_p} B + \partial_{\psi_p} \Phi \right] - \frac{1}{D} (1 - \rho_c g' - g \partial_{\psi_p} \alpha) \times \\ &\quad \left[(\mu + \rho_{\parallel}^2 B) \partial_{\theta} B + \partial_{\theta} \Phi \right] + \frac{1}{D} (q + \rho_c I' + I \partial_{\psi_p} \alpha) \left[(\mu + \rho_{\parallel}^2 B) \partial_{\theta} B + \partial_{\theta} \Phi \right] - \partial_t \alpha\end{aligned}\quad (3)$$

From Monte Carlo simulations, the local particle diffusion coefficient $D(v)$ was calculated for thermal ions starting at $r = a/2$ in a circular tokamak without islands, using the parameters $B_0 = 2T, R = 2m, a = 20cm, q = 4, T_e = T_i = 1keV$. As a benchmark they are compared with the neoclassical analytic expression for a tokamak [7], giving a good agreement (Fig. 2).

Figure 3 shows trajectory Poincaré plots for 20 keV ions in a single $m/n = 2/1$ island tokamak field. In Fig. 3a secondary $m = 3$ and $m = 5$ islands appear in the ion motion for a perturbation amplitude of 6×10^4 . In Fig. 3b the amplitude is 8×10^4 , which produces surface destruction. This leads to stochastic transport for a population of ions reaching these regions.

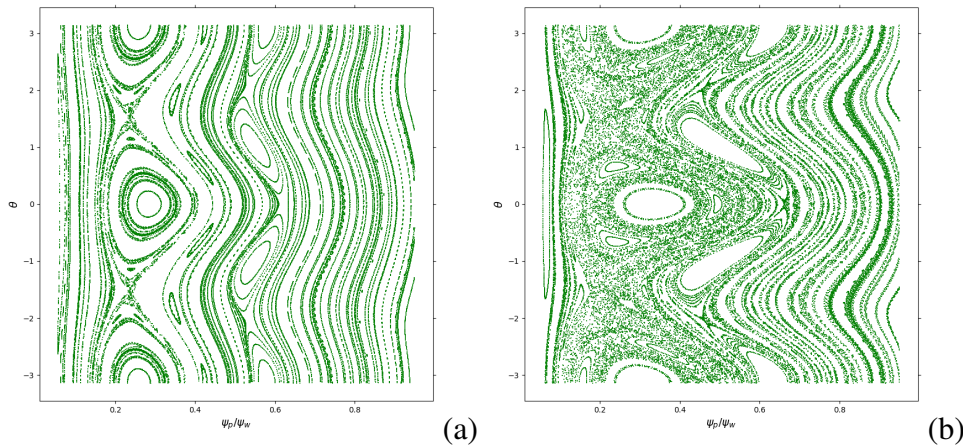


Figure 3: Poincaré plots of particle trajectories for amplitude (a) 6×10^4 , (b) 8×10^4 .

The distribution at 1 ms of 2000, 20 keV ions started at $r = 0.38a$ with pitch-angle $\lambda = 1$ is shown in Fig.4 for the two island amplitudes. It can be seen that there is a stochastic transport

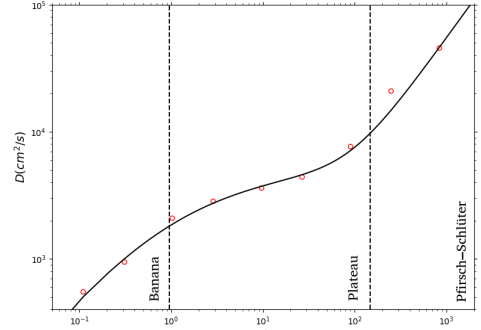


Figure 2: Neoclassical diffusion benchmark.

threshold between 6×10^4 and 8×10^4 .

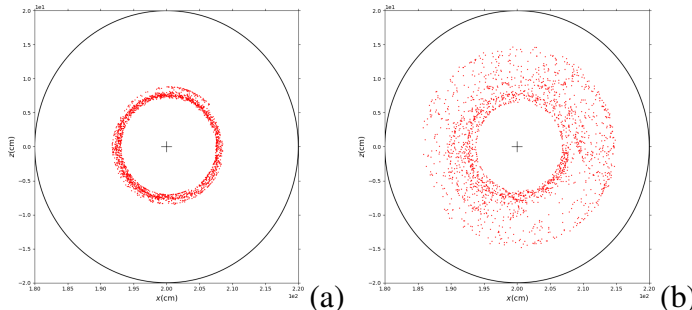


Figure 4: Final distribution with $\phi = 0$ (a) and $\phi = 8kV$ (b).

Eq. (2) with $\varepsilon_h = r^l$ [6]. Just as in the tokamak case, the equations of motion are (3) and collisions are introduced through (1). In this case orbits have the additional effect of helical trapping. Fig. 5 shows the particle and momentum dispersions. Ions were started at $r = 0.5a$ in the perturbed fields of a circular tokamak (top) and stellarator (bottom). Collisions in the plateau regime were included. The amplitude was chosen to be 8×10^4 , so there is surface destruction in the Poincaré plots of the particle trajectories. The diffusion coefficients computed from the slope do not have a significant change in the stellarator case with respect to the tokamak with values $D = 6 \times 10^2 \text{ cm}^2/\text{s}$.

V. Conclusions. In slab geometry, islands act as transport barriers. A radial electric field helps the confinement. For tokamak, there is destruction of surfaces in the particle Poincaré plots at a perturbation amplitude threshold for stochastic transport. Stochastic transport is a dominant effect over collisions. No significant change in transport was found in stellarators with respect to the tokamak case for the model chosen.

Acknowledgements. This work was partially supported by project DGAPA-UNAM IN112118.

References

- [1] MA Ochando, F Medina, et al. *Plasma Phys. Control. Fusion*, **45**, 221 (2003).
- [2] Andrés de Bustos Molina. PhD thesis, Universidad Complutense de Madrid (2013).
- [3] A. H. Boozer and G. Kuo-Petravic. *Phys. Fluids*, **24**, 851 (1981).
- [4] Roscoe B White. *The theory of toroidally confined plasmas*. World Scientific Publishing Company (2013).
- [5] R.B. White and M.S. Chance. *Phys. Fluids*, **27**, 2455 (1984).
- [6] H.E. Mynick, T.K. Chu, and A.H. Boozer. *Phys. Rev. Lett*, **48**, 322 (1982).
- [7] F.L. Hinton and R.D. Hazeltine. *Rev. Mod. Phys.*, **48**, 239 (1976).

The effect still appears when pitch-angle scattering is included. It is noticed that stochastic transport is a dominant feature over collisions.

IV. Stellarator model. The magnetic field for a stellarator with enhanced confinement is given by

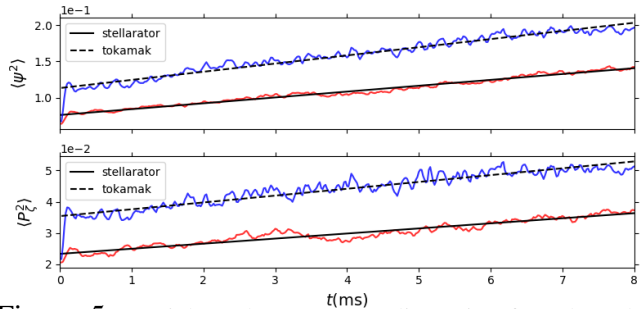


Figure 5: Particle and momentum dispersion for tokamak and stellarator.